Functional remodeling of gap junction-mediated electrical communication between adrenal chromaffin cells in stressed rats.

Claude Colomer, Luis A. Olivos Ore, Nathalie Coutry, Marie-Noëlle Mathieu, Sébastien Arthaud, Pierre Fontanaud, Irena Iankova, Françoise Macari, Erwan Thouennon, Laurent Yon, et al.

JN-RM-5597-07.R2, in press

Functional remodeling of gap junction-mediated electrical communication between adrenal chromaffin cells in stressed rats

Abbreviated title: chromaffin cell coupling in stressed rats

Claude Colomer[1,2,3,4], Luis A. Olivos Ore[1,2,3,4,5], Nathalie Coutry[1,2,3,4], Marie-Noëlle Mathieu[1,2,3,4], Sébastien Arthaud[6], Pierre Fontanaud[1,2,3,4], Irena Iankova[7], Françoise Macari[1,2,3,4], Erwan Thouënnon[6], Laurent Yon[6], Youssef Anouar[6] and Nathalie C. Guérineau[1,2,3,4]

[1]Institut of Functional Genomics, Montpellier, France; [2]CNRS UMR5203, Montpellier, France; [3]INSERM U661, Montpellier, France; [4]University of Montpellier (IFR3), Montpellier, France; [5]Department of Toxicology and Pharmacology, Complutense University of Madrid, Madrid, Spain; [6]INSERM U413, University of Rouen, Mont-Saint-Aignan, France; [7]INSERM U896, Montpellier, France

Correspondence and reprint requests should be addressed to Nathalie C. Guérineau, Institute of Functional Genomics, Department of Endocrinology, 141 rue de la Cardonille, 34094 Montpellier CEDEX 05, France. Tel: 33-4-67-14-29-59 ; Fax: 33-4-67-54-24-32 ; E-mail: nathalie.guerineau@igf.cnrs.fr

33 text pages, 8 figures, 2 tables

243 words in the abstract, 500 words in the introduction, and 1500 words in the discussion

Key words: gap junctional communication, connexins, nicotinic stimulation, cold exposure, dual patch-clamp, rat acute adrenal slices

Acknowledgments: We thank Drs. M.G. Desarménien, P.F. Méry, V. Homburger, A. Varrault and P. Mollard for helpful discussions in preparing the manuscript, D. Haddou, A. Carrette and P. Didier for technical assistance. We also thank N. Lautredou at the microscope facility of Montpellier RIO Imaging-Centre Régional d'Imagerie Cellulaire plateform. This work was supported by grants from Centre National de la Recherche Scientifique, Institut National de la Santé et de la Recherche Médicale, Ministère de l'Enseignement Supérieur et de la Recherche, Fondation pour la Recherche Médicale, ARC Régionale, Région Languedoc-Roussillon and Conseil Régional de Haute Normandie.

Conflict of interest statement: no conflict declared

Abstract

An increase in circulating catecholamine levels represents one of the mechanisms whereby organisms cope with stress. In the periphery, catecholamines mainly originate from the sympathoadrenal system. As we reported, in addition to the central control through cholinergic innervation, a local gap junction-delineated route between adrenal chromaffin cells contributes to catecholamine exocytosis. Here, we investigated whether this intercellular communication is modified when the hormonal demand is increased as observed during cold stress. Our results show that in cold exposed rats, gap junctional communication undergoes a functional plasticity, as evidenced by an increased number of dye-coupled cells. Of a physiological interest is that this up-regulation of gap junctional coupling results in the appearance of a robust electrical coupling between chromaffin cells that allows the transmission of action potentials between coupled cells. This enhancement of gap junctional communication parallels an increase in expression levels of connexin36 and connexin43 proteins. Both transcriptional and post-translational mechanisms are involved since Cx36 transcripts are increased in stressed rats and the expression of the scaffolding protein Zonula Occludens-1, known to interact with both Cx36 and Cx43, is also up-regulated. Consistent with an up-regulated coupling extent in stressed rats, the cytosolic Ca^{2+} concentration rises triggered in a single cell by an iontophoretic application of nicotine occur simultaneously in several neighboring cells. These results describe for the first time a functional plasticity of junctional coupling between adult chromaffin cells that should be crucial for adaptation to stress or sensitization to subsequent stressors.

Introduction

Stimuli which act as stressors elicit complex responses that enable an organism to cope with a changing environment and to respond effectively to a threat for its survival. Adaptative responses to stress are mediated by a synergistic activation of neuronal and neuroendocrine axis, *i.e.* the hypothalamo-pituitary-adrenocortical axis, the adrenomedullary hormonal system and the sympathetic noradrenergic system (Herman and Cullinan, 1997 ; Charmandari et al., 2005), but the relative intensity of their respective stimulation is stressor-specific (Goldstein and Kopin, 2007). Catecholamines are one of the primary mediators for many of the physiological consequences of the organism's response to stressors. In the adrenal medulla, the main peripheral tissue involved in catecholamine release, stress induces synthesis and release of catecholamines (Kvetnansky and Sabban, 1993), consistent with an increase in the activity of catecholamine biosynthetic enzymes (Sabban and Kvetnansky, 2001). Because an increase in catecholamine secretion is a key initial event in response to stressors, it is of interest to investigate how chromaffin cells behave to ensure increased catecholamine release in the blood circulation. *In vivo*, the secretion of catecholamines by chromaffin cells is chiefly controlled by the synaptic release of acetylcholine from splanchnic nerve terminals synapsing onto chromaffin cells (Douglas, 1968 ; Wakade, 1981). However, as reported by our group (Martin et al., 2001), in addition to this synaptic pathway, gap junction-mediated intercellular communication between chromaffin cells also contributes to catecholamine secretion and we proposed that junctional coupling may represent an efficient complement to synaptic neurotransmission to amplify catecholamine release. To date, whether the gap junction-delineated route can be modulated in response to stress remains unknown. Compelling evidence suggests that gap junctions might have a role in stress-induced rise in catecholamine secretion. First, gap junctions provide a widespread mechanism of intercellular dialogue by intercellular exchange of ions and metabolites and they can therefore signal the state of

activity of neighboring cells, thus allowing a coordinated multicellular response of the coupled cell clusters. Second, gap junction-dependent cell-cell cross-talk is a significant player of a variety of functions such as hormone secretion from endocrine/neuroendocrine tissues (Meda, 1996 ; Munari-Silem and Rousset, 1996 ; Hatton, 1997 ; Caton et al., 2002 ; Michon et al., 2005) including the adrenal medulla in which connexin36 and/or connexin43 have been reported to functionally connect chromaffin cells in situ (Martin et al., 2001). Third, in adrenal slices, gap junctional coupling efficiency between chromaffin cells is modulated by the sympatho-adrenal synaptic transmission (Martin et al., 2003).

These considerations prompted us to seek whether a stressful situation might modify the gap junctional communication between rat adrenal chromaffin cells. Our data indicate that, in response to a cold exposure for 5 days, gap junctional coupling is dramatically enhanced. We show the appearance of a robust electrical coupling between chromaffin cells resulting in a functional propagation of cell excitation. In parallel, Cx36 and Cx43 expression is up-regulated. We propose that these changes of cell-cell coupling may contribute to improvement of the stimulation-secretion coupling efficiency in the adrenal medulla, accounting for an increase in catecholamine secretion.

Material and methods

All procedures in this study conformed to the animal welfare guidelines of the European Community and were approved by the french Ministry of Agriculture (authorization no. 34.247).

Cold stress paradigm

Male Wistar rats (Janvier, Le Genest-St-Isle, France) were kept in plastic cages with bedding and continuously exposed to an ambient temperature of 4°C for 5 days. Control rats were housed in similar conditions but at 22°C. The rooms were maintained on a 12-hour light/dark

cycle (light on from 8 a.m. to 8 p.m.). Food and water were available *ad libitum*. The reversibility of cold stress-induced changes was assessed in rats housed in standard conditions for 5 days after stress cessation. The mean body weight of animals was similar at the beginning of treatment (control, 335 ± 22 g, n = 9; cold stress, 321 ± 14 g, n = 22, $P>0.01$), whereas control animals gained weight (11.8 ± 2.2 %) in contrast to stressed rats (-4.3 ± 4.6 %) over the 5 day period ($P<0.01$). Before testing, adrenals from control and stressed rats were also weighted and circulating and adrenal catecholamine levels were titrated.

Circulating and adrenal catecholamine assays

Rat decapitation was properly conducted by skilled staff, ensuring rapid death and sample collection. Catecholamine assays were conducted as previously reported (Grouzmann et al., 1994). Briefly, adrenal glands were sonicated in 0.1 M perchloric acid. The homogenate was centrifuged (10 min, 4°C, 3000 *g*), the supernatant collected and frozen until quantification. The pellets were used for measurement of protein concentrations by the Bradford method (Bradford, 1976). Aliquots of adrenal extract supernatants were injected into the HPLC system and quantified by electrochemical detection (Alexys 100 LC-EC System equipped with the Decade II detector, Antec Leyden, The Netherlands). Results were expressed in nmol norepinephrine or epinephrine per mg of protein. Trunk blood samples were collected in EDTA pre-coated tubes and centrifuged. Then, plasmas were frozen at -80°C until determination of circulating catecholamines. Norepinephrine and epinephrine were extracted on alumina and, as for adrenal extracts, measured by HPLC with electrochemical detection.

Adrenal slice preparation

Acute slices were prepared from rats as reported previously (Martin et al., 2001). After removal, the glands were kept in ice-cold saline for 2 min. A gland was next glued onto an agarose cube and transferred to the stage of a vibratome (DTK-1000, D.S.K, Dosaka EM CO. LTD, Kyoto, Japan). Slices of 250 μm thickness were then cut with a razor blade and

transferred to a storage chamber maintained at 37°C, containing Ringer's saline (in mM): 125 NaCl, 2.5 KCl, 2 $CaCl_2$, 1 $MgCl_2$, 1.25 NaH_2PO_4, 26 $NaHCO_3$, 12 glucose and buffered to pH 7.4. The saline was continuously bubbled with carbogen (95% O_2 / 5% $C0_2$).

Electrophysiology

All experiments were performed in the whole-cell configuration of the patch-clamp technique (Hamill et al., 1981). Patch pipettes were pulled to a resistance of 5-8 MΩ from borosilicate glass and filled with the following internal solution (in mM): 140 potassium-gluconate, 2 $MgCl_2$, 1.1 EGTA, 5 Hepes, that was titrated to pH 7.2 with KOH. Adrenal slices were transferred to a recording chamber attached to the stage of an upright microscope (Axioskop FS, Zeiss, Le Pecq, France) and continuously superfused with Ringer's saline at 34°C. Membrane potentials of chromaffin cell pairs were recorded under current-clamp conditions using an EPC-9 dual patch-clamp amplifier (HEKA Electronik, Lambrecht/Pfalz, Germany) and filtered at 3 kHz. The junctional current Ij was monitored under dual voltage-clamp conditions (Neyton and Trautmann, 1985). To calculate the macroscopic junctional conductance Gj, the I/V curve in which Ij amplitude was plotted as a function of the transjunctional voltage Vj was fitted by a computed linear regression $y = ax + b$ (where y corresponds to Ij and x to Vj). Gj was then given by the slope of the linear regression. Coupling ratios were calculated as the current amplitude in the nearby cell divided by the current amplitude in the stepped cell. Signals were analyzed with PulseFit 8.50 (HEKA Electronik).

Dye transfer assay

The fluorescent dye LY (Lucifer yellow-CH, lithium salt, 0.5 mM) was introduced into chromaffin cells using patch pipettes. Dye transfer between gap junction-coupled cells was visualized with confocal microscopy using the 488 nm-centered wavelength of the laser beam. The extent of LY diffusion was estimated by counting the number of neighboring cells that

received dye in 15 min. The probability of LY diffusion was expressed as a ratio corresponding to the number of injected cells that show dye transfer to adjacent cells over the total number of injected cells.

Confocal imaging of cytosolic calcium

Ca^{2+} changes were routinely monitored with a real-time (30-480 frames/s) confocal laser scanning microscope equipped with an Ar/Kr laser (Odyssey XL with InterVision 1.5.1 software, Noran Instruments Inc., Middleton, WI). Cells were viewed with a 63x 0.9 NA achroplan water immersion objective (Zeiss). The largest detection slit (100 μm) of the confocal microscope was used for $[Ca^{2+}]i$ measurements, giving bright images with a 3.1 μm axial resolution. Slices were loaded with the Ca^{2+}-sensitive fluorescent probe Oregon Green 488 BAPTA-1 by exposure to 0.5 μM Oregon Green 488 BAPTA-1 acetoxymethyl ester and Pluronic acid F127 (Invitrogen, Cergy Pontoise, France) for 40 min at 37°C. Oregon Green 488 BAPTA-1 was excited through a 488 nm-band-pass-filter and the emitted fluorescence was collected through a 515 nm-barrier filter. To follow the time course of Oregon Green 488 BAPTA-1 emission changes, the bright-over-time tool of the software package was applied to live images (120 images/s with averaging 4 frames). Because Oregon Green 488 BAPTA-1 is a single-wavelength dye, its emission is a function of both intracellular Ca^{2+} and dye concentrations. $[Ca^{2+}]i$ changes were expressed as the F/Fmin ratio where Fmin was the minimum fluorescence intensity measured during the recording. Acquired data and images were then processed for analysis with ImageJ 1.37 and Igor Pro 5.04 (Wavemetrics Inc., Lake Oswego, OR) software.

Iontophoretic application of nicotine

To mimick the *in vivo* release of transmitters into the synaptic cleft, the cholinergic secretagogue nicotine (nicotine chloride, 200 mM) was iontophoretically applied onto a single chromaffin cell *via* a sharp microelectrode, leading to focal stimulation of a single cell

(Martin et al., 2001). The concentration reported is that in the microelectrode. Nicotine was prepared from a stock solution in an acetate buffer (pH 4). At this pH value, nicotine was negatively charged and, consequently, could be delivered from the microelectrode upon application of outward current pulses (50 nA intensity, 10 ms duration).

Immunostaining

To process for connexin immunolabeling, adrenal glands were rapidly removed and frozen by immersion in liquid nitrogen. The glands were next mounted in Tissue-Tek® O.C.T. compound and cut into 10-20 μm-thick sections using a cryostat. Gland sections were mounted on coverslips and post-fixed at -20°C for 10 min in acetone and were incubated overnight with the following primary polyclonal antibodies, a rabbit anti-Cx36 or a rabbit anti-Cx43 (1:250, Zymed Laboratories, CliniSciences, Montrouge, France). Sections were then incubated 1h at room temperature with appropriate secondary antibodies conjugated to Alexa Fluor 488 (1:2000, Molecular Probes, Eugene, OR) or Cy3 (1:2000, Jackson ImmunoResearch Laboratories, Inc., West Grove, PA). Primary and secondary antibodies were diluted in PBS containing 2% BSA and 0.1% Triton X-100. Stained sections were imaged with a Biorad MRC-1024 confocal laser scanning microscope equipped with a krypton-argon mixed gas laser. The specificity of the commercial antibodies has been assessed by absorption tests. Negative controls were carried out by omitting primary antibodies.

Western blotting

After decapsulation, medullary tissue was separated from the cortex. To remove remaining cortical cells, samples were incubated for 10 min at 0-4°C in Ringer's saline containing 1 mg/ml collagenase type I. Membrane proteins were then isolated using lysis buffer (10 mM Tris-HCl, pH 7.4, 5 mM EDTA, 1 mM sodium orthovanadate and 10 mM NaF as phosphatase inhibitors, 10 mM β−glycerophosphate and 1% Triton X-100), supplemented with Mini

complete protease inhibitors (Roche Applied Science, Laval, Quebec). Proteins were centrifuged once for 5 min at 5,000 rpm and supernatants were collected. Proteins were centrifuged for 30 min at 13,200 rpm and concentrations were determinated using the Dc Protein Assay Kit (Bio-Rad Laboratories, Hercules, CA). Protein samples (15 μg) were heated for 5 min at 95°C and separated on a 10% polyacrylamide gel (7% for ZO-1 detection) in parallel with molecular weight markers. Electrophoresed proteins were transferred onto a nitrocellulose membrane (80 V, 60 min and 80 V, 75 min using a semi-dry blotting system (Bio-rad, Hercules, CA) for connexin and ZO-1 detection, respectively)**.** Blots were then blocked with 10% Blocking Reagent (BM Chemoluminescence Blotting Substrate kit, Roche Applied Science) in TBS (pH 7.4, 0.1% Tween 20) for 1 h at room temperature with gentle agitation. Blots were then incubated with the same polyclonal antibodies raised against Cx36 or Cx43 as those used for immunofluorescence, or a polyclonal rabbit anti-ZO-1 (1:250, Zymed Laboratories) in TBS-Tween 0.1% containing 10% Blocking Reagent at 4°C overnight. Following washout, blots were incubated with secondary antibodies peroxydase conjugated for 1 h at room temperature. This was followed by 1 min incubation in BM Chemoluminescence Blotting substrate. Labeled blots were then exposed to Fujifilm Medical X-Ray Film to visualize antibody binding. To ensure equal loading of protein samples, blots were stripped of their connexins or ZO-1 antibodies and reprobed with an actin-specific monoclonal antibody (actin, pan Ab-5, clone ACTN05, 1:1000, Interchim, Montluçon, France). Intensities of Cx36, Cx43 and ZO-1 bands were normalized to those of actin and quantified using ImageJ software.

Quantification of mRNA expression levels by real-time PCR

Total RNA was extracted from macrodissected adrenal medulla (same protocol as used for western blot experiments) and treated with DNase I using the RNeasy Micro extraction kit (Qiagen, Courtaboeuf, France). RNA (1 μg) was first reverse transcribed using Superscript III

reverse transcriptase (Invitrogen) and 250 ng of random hexamer (Amersham Biosciences Europe, Orsay, France) in a final volume of 20 µl. Real-time PCR analyses of *Cx36, Cx43* and housekeeping genes were performed using SYBR Green PCR master mix (Applied Biosystems, Foster City, CA) with 1:10 of the reverse-transcription reaction, and were carried out on an ABI 7500 Sequence Detector (Applied Biosystems). Primer sequences for *Cx36, Cx43* and housekeeping genes are given in Table 1. The concentration of the primers used was 300 nM each for *Cx43* and housekeeping genes, and 900 nM for *Cx36*. After an initial denaturation step for 10 min at 95°C, the thermal cycling conditions were 40 cycles at 95°C for 15 s and 60°C for 1 min. Each sample value was determined from triplicate measurements. The selection of appropriate housekeeping genes was performed with geNorm (Vandesompele et al., 2002). Expression of Cx36 and Cx43 transcripts was normalized to the geometric mean of the expression levels of three housekeeping genes, *Hprt* (hypoxanthine-guanine phosphoribosyltransferase), *GAPDH* (glyceraldehyde-3-phosphate dehydrogenase) and *Gus* (Glucuronidase), according to the formula Cx/geometric mean (R1, R2, R3) = $2^{-(Ct[Cx]-\text{arithmetic mean } [Ct(R1),Ct(R2),Ct(R3)])}$, where Ct is the threshold cycle, and R1, R2, R3 are the three reference genes.

Solutions and chemicals

Nicotine, Lucifer yellow (LY), collagenase type I, lectin from *Triticum vulgaris* and the gap junction blocker carbenoxolone were purchased from Sigma. Primers for qPCR were purchased from MWG-Biotech AG (Ebersberg, Germany).

Statistics

Numerical data are expressed as the mean ± SEM. Differences between groups were assessed by using the non-parametric Mann-Whitney U test. Unpaired Student's *t*-test was used to compare means. Percentages were compared using a contingency table and the chi-square test. Differences with $P<0.01$ were considered significant.

Results

As a validation of the cold stress paradigm, we measured adrenal weight and catecholamine content (intra-adrenal and in the blood circulation) and we found that these parameters were altered by the cold exposure. As reported by Kvetnansky and colleagues (1971), the adrenal weight was significantly increased (mean weight of the two adrenals for each rat 68.7 ± 3.2 mg, n = 9 *versus* 57.2 ± 1.6 mg, n = 9 for stressed and untressed rats, respectively, $P<0.01$). Consistent with enhanced synthesis and release of catecholamines commonly observed in response to a stressful situation (Kvetnansky et al., 1998), plasma levels of epinephrine and norepinephrine were also increased (by 44% and 36%, respectively, $P<0.01$, table 2). Concomitantly, the adrenal content of the two catecholamines was reduced by 25% for epinephrine and 38% for norepinephrine ($P<0.01$, table 2).

Appearance of gap junction-mediated robust electrical coupling between chromaffin cells in cold stressed rats

The effects of a 5-day cold exposure on gap junction-mediated cell-cell communication was investigated by imaging the diffusion of Lucifer yellow from a single patch-clamped chromaffin cell to neighbors. Both the percentage (82.2%, n = 382 *versus* 18.0%, n = 122 in controls) and the spreading extent of dye coupling between chromaffin cells (Figure 1A) were significantly up-regulated in cold stressed rats. While the spreading did not usually exceed 1-2 cells in controls, it could be extended to more than 2-4 cells in stressed animals (figure 1A, inset). To determine the functional relevance of this increased gap junctional communication, the membrane potential of chromaffin cell pairs was monitored in the whole-cell configuration of the dual patch-clamp technique (Figure 1B). Consistent with LY data, a significant electrical coupling evidenced by voltage changes reflected in the unstepped cell was recorded in 79.3% of cell pairs in stressed rats (n = 116) *versus* 24.1% in controls (n =

145) (P<0.01, Figure 1Ba). It is noteworthy that this increase in electrical coupling was fully reversible. Five days after cold stress cessation, the electrical coupling between chromaffin cells did not differ from the control condition (22.5%, n = 71 pairs *versus* 24.1%, n = 145 pairs in control, P>0.01, Figure 1Ba). Among cell pairs, the voltage changes in response to hyperpolarizing/depolarizing current injected into the stimulated cell were reflected as variably attenuated responses in the unstepped cell (Figures 1Bb and 1Bc). In all coupled cell pairs from control rats (n = 35), the action potential was distorted and led to a small depolarization in the coupled cell, thus indicating a weak coupling. However, in cold stressed rats, only a half of coupled pairs exhibited a weak coupling. In the remaining half, a robust coupling led to the transmission of suprathreshold responses resulting in action potentials. Taken together, these data strongly suggest the presence of two chromaffin cell populations, a weakly coupled cell population found in both control and cold stressed rats and a highly coupled cell population only found in stressed animals.

Biophysical properties of the electrical coupling were next investigated by recording macroscopic junctional currents (Ij) in chromaffin cell pairs voltage-clamped at -60 mV (Figure 2). Delivering voltage steps with command pulses of both polarities triggered Ij in the unstepped cell that displayed variable degree of attenuation (Figure 2A). Consistent with the presence of weakly and highly coupled chromaffin cell pairs in stressed rats, the coupling ratio exhibited a bimodal distribution over the range 0.02-0.97 (Figure 2B). When plotted as a function of the transjunctional potential, the I/V curve of Ij displayed a linear relationship within the membrane potential range of -60mV to +120 mV. The curve used to fit the data was derived from a linear regression, given a mean macroscopic junctional conductance Gj for weak coupling of 169 ± 10 pS and 248 ± 32 pS for control and stressed rats, respectively and 5.79 ± 0.56 nS for robust coupling in stressed rats (Figure 2C). In all cell pairs exhibiting

a coupling ratio value above 0.66 (*i.e.* as found in about 50% of coupled pairs in stressed rats) the evoked action potential was transmitted to the unstepped cell.

With the aim to examine whether electrical coupling was mediated by gap junctions, chromaffin cell pairs from control, cold exposed and rescued rats were recorded in the presence of the pharmacological decoupling agent carbenoxolone (Ishimatsu and Williams, 1996). Ij amplitude was continuously recorded before and during 15 min carbenoxolone bath application (Figure 3Aa). As expected for a current flowing through gap junction channels, Ij amplitude rapidly decreased upon carbenoxolone application whereas it remained unchanged in control saline. Carbenoxolone-induced full decoupling effect was observed within 15 min. The effect of carbenoxolone was partly reversible (about 50% within 10-12 min after washout, n = 4-8, Figure 3Ab). Consistent with a gap junction-mediated process, pretreatment with 100 μM carbenoxolone (15 min prior to recording) prevented the appearance of electrical coupling in pairs from control, cold exposed and rescued rats (Figure 3B).

Taken together, these results clearly show an up-regulation of gap junction-mediated chromaffin cell communication in the adrenal medulla of cold stressed rats, resulting in the appearance of a robust electrical coupling.

Up-regulation of connexin36 and connexin43 protein expression levels in cold stressed rats

We next conducted a series of experiments to characterize the mechanisms underlying the enhancement of junctional coupling in stressed rats. Gap junction function can be regulated at the transcriptional, translational and post-translational level (Oyamada et al., 2005). To determine whether connexin protein expression was modified in response to cold stress, immunofluorescent stainings using antibodies raised against Cx36 and Cx43 were performed on adrenal gland cryosections (Figure 4). A typical punctate fluorescence was observed for

both connexins in control and stressed rats. However, the labeling of both Cx36 and Cx43 appeared more abundant in cold stressed as compared to unstressed animals. In addition, Cx36-containing gap junction plaques seemed larger in size (Figure 4A, insets). To go further, membrane content of Cx36 and Cx43 was measured by western blot. Consistent with our immunofluorescent data, Cx36 and Cx43 protein levels were up-regulated in stressed rats (Figure 5A). To analyse the data, the levels of Cx36 and Cx43 were normalized to those of actin used as a loading control. Quantitative analysis summarized in figure 5B indicates a 3- and 2-fold increase for Cx36 and Cx43, respectively ($P<0.01$).

Several mechanisms, which are not mutually exclusive, could account for cold stress-induced increase in connexin levels. It may be a consequence of increased synthesis, increased stability at the plasma membrane and/or decreased degradation. As a first step towards the characterization of the mechanisms involved in increased connexin expression in cold exposed rats, we examined by real-time PCR whether the expression level of Cx36 and Cx43 transcripts was modified (data not shown). Total RNA was extracted from macrodissected adrenal medulla from 8 control and 8 cold exposed rats. Expression of connexin mRNA was normalized to the geometric mean of the expression levels of *Hprt*, *GAPDH* and *Gus* mRNA. Cx36 mRNA relative expression level was 2.5-fold higher in stressed rats (21.0 ± 6.5 *versus* 8.4 ± 1.5 in stressed and control rats, respectively, $P<0.05$). No change was observed for Cx43 transcripts (relative expression 14746 ± 1193 *versus* 14517 ± 1565 for stressed and control rats, respectively, $P>0.05$), thus indicating that other mechanisms were involved. We therefore addressed the involvement of post-translational changes such as stability of gap junctional plaques. Anchored gap junctions at the plasma membrane are reported to bind to scaffolding proteins, such as Zonula Occludens-1 (ZO-1). This PDZ domain-containing protein has been shown to interact with various connexins including Cx36 and Cx43 (Giepmans and Moolenaar, 1998 ; Li et al., 2004). Although ZO-1

function at the gap junction still remains elusive, it has been suggested that ZO-1 may contribute to the assembly and/or stability of gap junctions (Laing et al., 2005 ; Singh et al., 2005). As illustrated in figure 6, ZO-1 expression is up-regulated in cold stressed rats and densitometric analysis of immunoblots indicates that ZO-1 expression level is 2-fold higher in stressed rats ($P<0.01$, as compared with unstressed rats).

Physiological relevance of increased gap junctional coupling

Increased spontaneous $[Ca^{2+}]i$ co-activity between chromaffin cells in cold stressed rats

Because gap junction-mediated cell-cell communication can support synchronous activity between endocrine/neuroendocrine cells (Guérineau et al., 1998 ; Martin et al., 2001), we imaged spontaneous changes in cytosolic Ca^{2+} concentration ($[Ca^{2+}]i$) in chromaffin cell clusters using real-time confocal microscopy. Co-active cell clusters were found both in slices from control and cold stressed rats, but in the latter, the occurrence was significantly higher (72.5%, n = 69 recorded cell fields *versus* 43.9%, n = 41 in control rats, $P<0.01$, Figure 7). However, the extent of spontaneous $[Ca^{2+}]i$ co-activity did not differ between control and stressed rats and appeared to be restricted to a limited number of cells (2-3 on the same optical plane). To determine whether gap junctional coupling was involved in the co-activity process, spontaneous $[Ca^{2+}]i$ changes in stressed rats were recorded in carbenoxolone-containing saline (100 µM, 15 min before testing). As shown in the histogram, co-active cell clusters occurred less frequently than in control conditions ($P<0.01$).

Extended nicotine-induced synchronous multicellular $[Ca^{2+}]i$ increases in cold stressed rats

As reported (Martin et al., 2001), the gap junction-delineated route between adrenal chromaffin cells allows synchronous multicellular $[Ca^{2+}]i$ responses after nicotinic stimulation. What are the consequences of an up-regulated electrical coupling on nicotine-

induced synchronous Ca^{2+} signalling in chromaffin cell clusters in cold stressed rats? To address this issue, nicotine-evoked changes in $[Ca^{2+}]i$ in chromaffin cells were imaged in both control and cold exposed rats. Only cell fields in which the iontophoretic application of nicotine triggered a Ca^{2+} response in the stimulated cell were taken into consideration. In control slices, simultaneous transient $[Ca^{2+}]i$ rises were observed in 63% of stimulated cell clusters (n = 27) and the extent of co-activity was mainly restricted to 1-2 adjoining cells (Figure 8A, left panel and Figure 8B, open bars). By contrast, in 81.8 % of tested cell clusters (n = 55) in stressed rats, a large number of chromaffin cells (up to 11 in the same optical focus) displayed simultaneous $[Ca^{2+}]i$ co-activity in response to nicotine iontophoresis (Figure 8A, right panel and Figure 8B, filled bars). The propagated signal between chromaffin cells reliably persisted upon repetitive applications of nicotine, indicating that the intercellular mechanism underlying the propagation did not desensitize during the recording time (data not shown). To determine whether gap junctions were involved in the $[Ca^{2+}]i$ co-activity process, similar experiments were carried out in stressed rats in the presence of carbenoxolone. Bath-applied carbenoxolone (100 μM, 15 min before testing) significantly reduced the occurrence of spontaneous co-activation between adjacent chromaffin cells (10.6%, n = 47 *versus* 72.5%, n = 69 in the presence and in the absence of carbenoxolone, respectively, $P<0.01$, data not shown). Additionally, the iontophoretic nicotine application (10 ms) triggered simultaneous $[Ca^{2+}]i$ co-activity only in 16.7% of stimulated clusters (n = 24), compared to 81.8% without carbenoxolone (Figure 8C, $P<0.01$). As previously reported (Martin et al., 2001), carbenoxolone modified neither the percentage of spontaneously active cells nor the amplitude and duration of the nicotine-activated Ca^{2+} response (data not shown). Another set of data further confirmed the involvement of gap junctions. First, the calculation of the speed of nicotine-induced signal propagation, based on a 20 μm distance between adjacent chromaffin cell centers in rat (Martin et al., 2001), is consistent with a gap junctional-

mediated pathway (716 ± 52 μm/s, n = 124 *vs* 435 ± 49 μm/s, n = 31, $P<0.01$). Second, as control experiments of iontophoretic application of nicotine, we showed that current polarity inversion (n = 18) or application of nicotine-free saline (n = 11) never induced $[Ca^{2+}]i$ changes in either stimulated or adjacent cells. Moreover, extracellular diffusion of nicotine could reasonably be ruled out since i) a $[Ca^{2+}]i$ increase was not observed in all cells belonging to the same cluster, while all these cells were sensitive to pressure ejection of nicotine and ii) in some experiments, only the stimulated cell exhibited a $[Ca^{2+}]i$ rise.

These results point **out** the functional role played by gap junctional communication in the expression of synchronized Ca^{2+} signals between chromaffin cells, in particular in cold stressed rats.

Discussion

This study reports a functional remodeling of gap junction-mediated intercellular communication in the adult rat adrenal medulla in response to cold stress. The increased electrical coupling between chromaffin cells likely contributes to improve the stimulus-secretion coupling efficiency and may therefore represent one of the endogenous mechanisms by which the medulla ensures appropriate sustained catecholamine secretion in response to stressful conditions.

Appearance of a robust electrical coupling in cold stressed rats: a functional support for coordinating multicellular $[Ca^{2+}]i$ rises between chromaffin cells

We show that a persistent cold exposure induces a robust electrical coupling between chromaffin cells. Two populations of electrically coupled cells can be distinguished in stressed rats, based on junctional conductance values. While a weak coupling allows small depolarizations to propagate upon action potential firing, a robust coupling triggers action

potentials in the coupled cells. The contribution of Cx36- and/or Cx43-built channels to weak *versus* robust coupling is unknown but, because connexin channels exhibit different voltage sensitivities (Gonzalez et al., 2007), their roles in propagating electrical signals between adjacent cells likely differ. The weak voltage dependence of Cx36 channels suggests that electrical coupling may not be disrupted during secretagogue-mediated action potential discharges. By contrast, Cx43 channels that are highly voltage-sensitive may predominantly be regulated during firing. Cold stress induces an increased expression of both Cx36 and Cx43 proteins but by different mechanisms since only Cx36 mRNA is up-regulated. The fact that some cells co-express both mRNAs (Martin et al., 2001) supports the hypothesis that chromaffin cells might express both connexins and regulate their synthesis differently. Alternatively, two cell populations may exist, expressing either Cx36 or Cx43 under different conditions. A possibility would then be that stress leads to an up-regulation of one population. Only a double electron microscopy study would reliably address this issue.

We show that occurrence of the highly coupled cell population in cold stressed rats correlates with long-distance activation of simultaneous $[Ca^{2+}]i$ increases in coupled cells. The high speed of $[Ca^{2+}]i$ co-activation between chromaffin cells in response to nicotinic stimulation of a single cell likely results from gap junction-mediated propagation of a depolarizing wave. Although we cannot definitively rule out the involvement of other communication modes (such as paracrine action of factors co-released with catecholamines), gap junctions likely represent the anatomical correlate of the functional coupling observed here. Several observations support this proposal: i) propagation of electrical events between two adjacent cells, ii) junctional current recorded in cell pairs and iii) carbenoxolone-induced reduction of junctional currents and simultaneous $[Ca^{2+}]i$ changes upon nicotinic stimulation.

As reported for pancreatic beta-cells in which gap junctional coupling provides the basis for coordinating agonist-induced $[Ca^{2+}]i$ oscillations (Calabrese et al., 2003), it is likely that

the extended electrical activity propagation through robustly coupled chromaffin cells supports multicellular [Ca^{2+}]i co-activities within cell clusters. Moreover, our data strongly support the postulate that propagation of action potentials between chromaffin cells *via* electrotonic coupling may amplify the secretory signal to ensure massive catecholamine release in the intact gland (Ceña et al., 1983). Because propagation of electrical signals and associated [Ca^{2+}]i transients is more efficient between highly coupled cells than between weakly coupled cells, we propose that the robust coupling has a strong influence on the stimulus-secretion coupling and may account for the enhancement of plasma catecholamine levels found in cold exposed rats (Kvetnansky et al., 1971).

Long-term persistence of changes in gap junction-mediated communication

In addition to short-term changes, gap junctional coupling also undergoes long-term plasticity associated with functional changes that can persist for weeks (Chang et al., 2000 ; Martin et al., 2003). Modulation of connexin expression at the transcriptional level (Oyamada et al., 2005), connexin assembly into functional channels, modification of existing gap junction plaques (Chang et al., 2000) and/or steps affecting connexon number or trafficking (Martin et al., 2003) are possible targets involved in persistent changes of gap junctional communication.

What cellular mechanisms could account for the sustained change in gap junctional coupling strength observed in cold stressed rats? Our data indicate that both transcriptional and post-translational mechanisms are involved, depending on the connexin. The enhancement of cell coupling in stressed rats parallels an increase in number of Cx36 and Cx43-built gap junctions, as found in pancreatic beta-cells in response to a stimulation of insulin release (Collares-Buzato et al., 2001). A means to control junctional communication is the modulation of connexin life cycle and stability at the plasma membrane. This occurs through interaction with a variety of scaffolding proteins (Hervé et al., 2007) that can act by

preventing interaction with degradation machinery or by forming complexes between connexins and the cytoskeleton (Butkevich et al., 2004). Our results showing that ZO-1 expression level, a scaffolding protein interacting with both Cx36 and Cx43 (Giepmans and Moolenaar, 1998 ; Li et al., 2004) is up-regulated in stressed rats are in agreement with our proposal that Cx36 and/or Cx43 may be stabilized at the plasma membrane, leading to a slowdown of connexin turn-over. Consistent with this hypothesis is the demonstration that i) Cx43 turns over at a more rapid rate when it no longer interacts with ZO-1 (Toyofuku et al., 2000), ii) disruption of the association between Cx43 and ZO-1 reduces junctional communication and iii) transfer of Cx43 to the plasma membrane is affected by changes in the abundance of ZO-1 (Laing et al., 2005). Alternatively, interaction between ZO-1 and Cx36/Cx43 may modify their trafficking and/or facilite their interactions with other proteins. As shown by qPCR experiments and reported for genes encoding catecholamine-synthesizing enzymes and related transcription factors (Baruchin et al., 1990 ; Sabban and Kvetnansky, 2001 ; Sabban et al., 2006), mechanisms taking place at the transcriptional level can also be involved. We show that in cold stressed rats, Cx36 protein expression level faithfully parallels Cx36 mRNA expression level, as opposed to Cx43 for which mRNA expression level remains unchanged. Whether or not other connexin-related genes are affected remains unknown.

In the adrenal medulla, the degree of junctional coupling between chromaffin cells is also under a tonic control exerted by cholinergic synaptic inputs (Martin et al., 2003). Because the sympatho-adrenal system is activated during cold stress, one could propose that synaptically-released factors might acutely and chronically modulate intercellular coupling (Hatton, 1998). To address this issue, further experiments conducted in denervated adrenals are required. Activation of the hypothalamo-pituitary-corticoadrenal axis is also an important component of the stress response. Because cortical and medullary tissues interact with each other (Einer-Jensen and Carter, 1995 ; Bornstein et al., 1997), gap junctional coupling

between chromaffin cells could be regulated by factors released from the cortex such as adrenocorticotropin, reported to increase Cx43-mediated communication (Murray et al., 2003). Although we cannot definitively rule out the involvement of cortical factors in cold stress-induced increased junctional coupling, it is noteworthy that a cold exposure induces only a weak activation of the hypothalamo-pituitary-adrenocortical axis (Pacak et al., 1995).

Physiological relevance of up-regulated connexin expression in stressed rats: increased stimulation-secretion coupling efficiency

The up-regulation of gap junctional coupling in cold stressed rats results in an increase in both spontaneous and nicotine-evoked simultaneous $[Ca^{2+}]i$ rises between chromaffin cells. Because $[Ca^{2+}]i$ rise is a prerequisite for exocytosis and since cell-cell communication contributes to catecholamine release (Martin et al., 2001), we propose that the increased gap junctional coupling described here in cold stressed rats is physiologically relevant in terms of catecholamine secretion. Further experiments are required to definitively assess the causal link between up-regulated gap junctional coupling and increased secretory function. With regard to neuroendocrine secretion, an increase in number and expression of gap junctions has also been reported in beta-cells in response to stimulation of insulin release (Collares-Buzato et al., 2001). In addition, during maturation of neonatal pancreatic islets, the gain of capacity of the islet to secrete insulin is associated with an increased Cx36 expression (Leite et al., 2005). Moreover, it is noteworthy that an increased gap junctional communication between chromaffin cells has been also found in rats exposed to a restraint stress (C. Colomer and N.C. Guérineau, unpublished observations). Our data demonstrate that, among adaptative responses to stress, increase in catecholamine secretion is associated with an up-regulation of gap junctional communication between chromaffin cells. Gap junction expression in numerous tissues prompts us to hypothesize that this unanticipated role of gap junctional coupling might

be extended to other stress-responsive tissues and, more generally, that an up-regulation of gap junctional communication between neuroendocrine/endocrine cells might be a general mechanism whereby secretory tissues dynamically adapt to increased hormonal demands.

Another interesting outcome of our data deals with the influence of prior experience with the homotypic/heterotypic stressor on the reactivity of adrenomedullary system to subsequent stress. As reported (Ma and Morilak, 2005 ; Sabban and Serova, 2007), cold stress exposure sensitizes catecholaminergic systems of the adrenal medulla and the locus coeruleus. An up-regulated gap junctional communication between chromaffin cells might be one endogenous mechanism whereby the adrenomedullary system is sensitized. Such functional sensitization could be an important component for stress adaptation and may also contribute to dysregulation of the stress response.

References

Baruchin A, Weisberg EP, Miner LL, Ennis D, Nisenbaum LK, Naylor E, Stricker EM, Zigmond MJ, Kaplan BB (1990) Effect of cold exposure on rat adrenal tyrosine hydroxylase: an analysis of RNA, protein, enzyme activity and co-factor levels. J Neurochem 54:1769-1775.

Bornstein SR, Ehrhart-Bornstein M, Scherbaum WA (1997) Morphological and functional studies of the paracrine interaction between cortex and medulla in the adrenal gland. Microsc Res Tech 36:520-533.

Bradford MM (1976) A rapid and sensitive method for the quantitation of microgram quantities of protein utilizing the principle of protein-dye binding. Anal Biochem 72:248-254.

Butkevich E, Hulsmann S, Wenzel D, Shirao T, Duden R, Majoul I (2004) Drebrin is a novel connexin-43 binding partner that links gap junctions to the submembrane cytoskeleton. Curr Biol 14:650-658.

Calabrese A, Zheng M, Serre-Beinier V, Caton D, Mas C, Satin LS, Meda P (2003) Connexin36 controls synchronization of Ca^{2+} oscillations and insulin secretion in MIN6 cells. Diabetes 52:417-424.

Caton D, Calabrese A, Mas C, Serre-Beinier V, Wonkam A, Meda P (2002) Beta-cell crosstalk: a further dimension in the stimulus-secretion coupling of glucose-induced insulin release. Diabetes Metab 28:3S45-3S53.

Ceña V, Nicolas GP, Sanchez-Garcia P, Kirpekar SM, Garcia AG (1983) Pharmacological dissection of receptor-associated and voltage-sensitive ionic channels involved in catecholamine release. Neuroscience 10:1455-1462.

Chang Q, Pereda A, Pinter MJ, Balice-GordonRJ (2000) Nerve injury induces gap junctional coupling among axotomized adult motor neurons. J Neurosci 20:674-684.

Collares-Buzato CB, Leite AR, Boschero AC (2001) Modulation of gap and adherent junctional proteins in cultured neonatal pancreatic islets. Pancreas 23:177-185.

Einer-Jensen N, Carter AM (1995) Local transfer of hormones between blood vessels within the adrenal gland may explain the functional interaction between the adrenal cortex and medulla. Med Hypotheses 44:471-474.

Giepmans BN, Moolenaar WH (1998) The gap junction protein connexin43 interacts with the second PDZ domain of the zona occludens-1 protein. Curr Biol 8:931-934.

Goldstein DS, Kopin IJ (2007) Evolution of concepts of stress. Stress 10:109-120.

Gonzalez D, Gomez-Hernandez JM, Barrio LC (2007) Molecular basis of voltage dependence of connexin channels: an integrative appraisal. Prog Biophys Mol Biol 94:66-106.

Grouzmann E, Werffeli-George P, Fathi M, Burnier M, Waeber B, Waeber G (1994) Angiotensin-II mediates norepinephrine and neuropeptide-Y secretion in a human pheochromocytoma. J Clin Endocrinol Metab 79:1852-1856.

Guérineau NC, Bonnefont X, Stoeckel L, Mollard P (1998) Synchronized spontaneous Ca^{2+} transients in acute anterior pituitary slices. J Biol Chem 273:10389-10395.

Hamill OP, Marty A, Neher E, Sakmann B, Sigworth FJ (1981) Improved patch-clamp techniques for high-resolution current recording from cells and cell-free membrane patches. Pflügers Arch 391:85-100.

Hatton GI (1997) Function-related plasticity in hypothalamus. Annu Rev Neurosci 20:375-397.

Hatton GI (1998) Synaptic modulation of neuronal coupling. Cell Biol Int 22:765-780.

Herman JP, Cullinan WE (1997) Neurocircuitry of stress: central control of the hypothalamo-pituitary-adrenocortical axis. Trends Neurosci 20:78-84.

Hervé JC, Bourmeyster N, Sarrouilhe D, Duffy H (2007) Gap junctional complexes: from partners to functions. Prog Biophys Mol Biol 94:29-64.

Ishimatsu M, Williams JT (1996) Synchronous activity in locus coeruleus results from dendritic interactions in pericoerulear regions. J Neurosci 16:5196-5204.

Kvetnansky R, Gewirtz GP, Weise VK, Kopin IJ (1971) Catecholamine-synthesizing enzymes in the rat adrenal gland during cold exposure. Am J Physiol 220:928-931.

Kvetnansky R, Sabban EL (1993) Stress-induced changes in tyrosine hydroxylase and other catecholamine biosynthetic enzymes. In: Tyrosine hydroxylase: from discovery to cloning (Naoi M, Parvez SH, eds), pp253-281. VSP Press, Utrecht.

Kvetnansky R, Pacak K, Sabban EL, Kopin IJ, Goldstein DS (1998) Stressor specificity of peripheral catecholaminergic activation. In: Advances in Pharmacology (Goldstein DS, Eisenhofer G, McCarty R, eds), pp556-560. Academic Press, San Diego, CA.

Laing JG, Chou BC, Steinberg TH (2005) ZO-1 alters the plasma membrane localization and function of Cx43 in osteoblastic cells. J Cell Sci 118:2167-2176.

Leite AR, Carvalho CP, Furtado AG, Barbosa HC, Boschero AC, Collares-Buzato CB (2005) Co-expression and regulation of connexins 36 and 43 in cultured neonatal rat pancreatic islets. Can J Physiol Pharmacol 83:142-151.

Li X, Olson C, Lu S, Nagy JI (2004) Association of connexin36 with zonula occludens-1 in HeLa cells, betaTC-3 cells, pancreas, and adrenal gland. Histochem Cell Biol 122:485-498.

Ma S, Morilak DA (2005) Chronic intermittent cold stress sensitises the hypothalamic-pituitary-adrenal response to a novel acute stress by enhancing noradrenergic influence in the rat paraventricular nucleus. J Neuroendocrinol 17:761-769.

Martin AO, Mathieu M-N, Chevillard C, Guérineau NC (2001) Gap junctions mediate electrical signaling and ensuing cytosolic Ca^{2+} increases between chromaffin cells in adrenal slices: a role in catecholamine release. J Neurosci 21:5397-5405.

Martin AO, Mathieu M-N, Guérineau NC (2003) Evidence for long-lasting cholinergic control of gap junctional communication between adrenal chromaffin cells. J Neurosci 23:3669-3678.

Meda P (1996) The role of gap junction membrane channels in secretion and hormonal action. J Bioenerg Biomembr 28:369-377.

Michon L, Nlend Nlend R, Bavamian S, Bischoff L, Boucard N, Caille D, Cancela J, Charollais A, Charpantier E, Klee P, Peyrou M, Populaire C, Zulianello L, Meda P (2005) Involvement of gap junctional communication in secretion. Biochim Biophys Acta 1719:82-101.

Munari-Silem Y, Rousset B (1996) Gap junction-mediated cell-to-cell communication in endocrine glands-molecular and functional aspects: a review. Eur J Endocrinol 135:251-264.

Murray SA, Davis K, Gay V (2003) ACTH and adrenocortical gap junctions. Microsc Res Tech 61:240-246.

Neyton J, Trautmann A (1985) Single-channel currents of an intercellular junction. Nature 317:331-335.

Oyamada M, Oyamada Y, Takamatsu T (2005) Regulation of connexin expression. Biochim Biophys Acta 1719:6-23.

Pacak K, Palkovits M, Kvetnansky R, Yadid G, Kopin IJ, Goldstein DS (1995) Effects of various stressors on in vivo norepinephrine release in the hypothalamic paraventricular nucleus and on the pituitary-adrenocortical axis. Ann N Y Acad Sci 771:115-130.

Sabban EL, Kvetnansky R (2001) Stress-triggered activation of gene expression in catecholaminergic systems: dynamics of transcriptional events. Trends Neurosci 24:91-98.

Sabban EL, Liu X, Serova L, Gueorguiev V, Kvetnansky R (2006) Stress triggered changes in gene expression in adrenal medulla: transcriptional responses to acute and chronic stress. Cell Mol Neurobiol 26:845-856.

Sabban EL, Serova LI (2007) Influence of prior experience with homotypic or heterotypic stressor on stress reactivity in catecholaminergic systems. Stress 10:137-143.

Singh D, Solan JL, Taffet SM, Javier R, Lampe PD (2005) Connexin 43 interacts with zona occludens-1 and -2 proteins in a cell cycle stage-specific manner. J Biol Chem 280:30416-30421.

Toyofuku T, Akamatsu Y, Zhang H, Kuzuya T, Tada M, Hori M (2000) c-Src regulates the interaction between connexin-43 and ZO-1 in cardiac myocytes. J Biol Chem 276:1780-1788.

Vandesompele J, De Preter K, Pattyn F, Poppe B, Van Roy N, De Paepe A, Speleman F (2002) Accurate normalization of real-time quantitative RT-PCR data by geometric averaging of multiple internal control genes. Genome Biol 3, RESEARCH0034.

Wakade AR (1981) Studies on secretion of catecholamines evoked by acetylcholine or transmural stimulation of the rat adrenal gland. J Physiol 313:463-480.

Figure legends

Figure 1: Up-regulation of metabolic and electrical coupling between chromaffin cells in cold stressed rats

A, The fluorescent dye was introduced into a single chromaffin cell by passive diffusion through a patch-clamp pipette. In stressed rats, the extent of LY spreading was significantly increased. The inset examplifies a LY diffusion to at least 4 neighboring cells in a cold exposed rat. Ba, Stress-induced reversible up-regulation of electrical coupling (*, $P<0.01$ as compared to control rats). Membrane potential was monitored in chromaffin cell pairs using the dual patch-clamp technique. Bb, Appearance of a robust coupling in stressed rats. Cells were current-clamped at -60 mV and hyperpolarizing/depolarizing steps (50 ms duration) were evoked in cell 1 (1*). The resulting voltage changes in the unstepped cell (cell 2) consisted either in small membrane hyperpolarization/depolarization (found in both control and stressed rats) or in transmission of the action potential (found only in stressed rats). Bc, Histogram illustrating that the robust coupling is present in about 50% of coupled chromaffin cell pairs in stressed rats.

Figure 2: Junctional currents recorded in chromaffin cell pairs from control and cold stressed rats

A, Representative chart recordings of junctional currents Ij in one control and two stressed (a weakly coupled and an highly coupled) cell pairs voltage-clamped at -60 mV (hyperpolarizing voltage step at -120 mV and depolarizing step at +40 mV, 150 ms duration). The asterisk marks the stimulated cell. B, Histograms illustrating the distribution range of the coupling

ratio (from 0 for non-coupled pairs to 1 for highly coupled pairs) calculated from voltage-clamp measurements of Ij (holding potential -60 mV, transjunctional potential from -120 to +60 mV, 150 ms duration). C, Pooled data of the macroscopic junctional conductance Gj showing the presence of two chromaffin cell populations exhibiting either low Gj (mean ~200pS) or high Gj (mean ~5 nS). Note that this latter is present only in stressed rats. The number of recorded cell pairs for each condition is indicated in parentheses.

Figure 3: Reversible inhibition of electrical coupling by the gap junctional blocker carbenoxolone

A, Time course of the blocking effect of carbenoxolone on Ij. Aa, Ij amplitude was continuously monitored in a chromaffin cell pair (stressed rat) voltage-clamped at -60 mV prior to and during bath-application of carbenoxolone (10-15 minutes). A voltage step (+40 mV, 150 ms) was elicited every minute. Carbenoxolone gradually decreased Ij amplitude leading to a complete blockade within a few minutes. Note the constant Ij amplitude during 20 minutes in control saline. Ab, Partial recovery of Ij amplitude after carbenoxolone washout. B, Fifteen minute-incubation with saline-containing carbenoxolone (100 μM) dramatically reduced the percentage of electrically coupled chromaffin cells, in both control, stressed and rescued rats. *, $P<0.01$ as compared to values in the absence of carbenoxolone. The number of recorded cell pairs is indicated in parentheses.

Figure 4: Immunofluorescent labeling of Cx36 and Cx43 in the adrenal medulla

Regular punctate appearance of Cx36 (A) and Cx43 (B) staining. For both connexins, the labeling was denser in stressed rats compared with control. Insets : higher magnification. In particular, note the presence of large fluorescent areas for Cx36 immunoreactivity (arrowheads).

Figure 5: Connexin 36 and connexin 43 protein expression levels are up-regulated in cold stressed rats

Connexin expression levels were measured by western blot. A, Representative immunoblots showing specific detection of Cx36 and Cx43 in the adrenal medulla of control and stressed rats. Actin was used as internal loading control. B, Histogram summarizing the densitometric analysis of immunoblots (normalized by actin) from 7 control and 7 stressed rats. Quantitative analysis shows that Cx36 and Cx43 expression was significantly increased in stressed rats (3- and 2-fold increase, respectively). *, $P<0.01$ as compared with unstressed rats.

Figure 6: Increased ZO-1 expression level in adrenal medulla of cold stressed rats

Immunoblot illustrating the up-regulation of ZO-1 expression level in stressed rats (n = 6) as compared with unstressed rats (n = 6).

Figure 7: Spontaneous $[Ca^{2+}]i$ co-activity in chromaffin cell doublets

Real-time spontaneous $[Ca^{2+}]i$ changes were imaged in Oregon Green 488 BAPTA-1-loaded adrenal slices. Chromaffin cell from both control and stressed rats exhibited synchronized co-activities that did not exceed cell doublets or triplets. The histogram shows that spontaneously co-active cell clusters occurred more frequently in stressed rats. Note that the percentage of spontaneous co-active cell clusters is dramatically reduced in carbenoxolone-containing saline (100 μM, 15 min before testing).

Figure 8: Extended nicotine-induced simultaneous $[Ca^{2+}]i$ increases between chromaffin cells in cold stressed rats

A, Nicotine (200 mM, 10 ms) was iontophoretically applied on cell 1* through a sharp microelectrode (the onset of the nicotinic stimulation is indicated by an arrow) and $[Ca^{2+}]i$

changes were imaged using real-time confocal microscopy. In a control rat (left panel), the $[Ca^{2+}]i$ increase originating in the stimulated cell was simultaneously detected in one adjacent cell while in a stressed rat, simultaneous $[Ca^{2+}]i$ increases were recorded into up to 6 adjacent cells (right panel). B, Extented co-activity of nicotine-triggered $[Ca^{2+}]i$ rises in stressed rats compared with untressed rats. C, Significant reduction of nicotine-induced $[Ca^{2+}]i$ co-activities in non-stimulated cells in the presence of the gap junction blocker carbenoxolone (100 μM, 15 min bath-application prior to recording).

Table 1: Primer sequences used for quantitative PCR

	forward sequence (5'-3')	reverse sequence (5'-3')
rCx36	AGACCACCGGGTAGAGTGACAA	GCAGGAAGGGCCACGAA
rCx43	CCCGACGACAACCAGAATG	TGGCTAATGGCTGGAGTTCAT
rGus	CACCACTGAGAGTAACAGGAAACAA	TCGTTGGCAATCCTCCAGTATCT
rHprt	TGACTATAATGAGCACTTCAGGGATT	TCGCTGATGACACAAACATGATT
rGAPDH	ATGATTCTACCCACGGCAAG	CTGGAAGATGGTGATGGGTT

Table 2: Effect of exposure to cold on plasma and adrenal epinephrine and norepinephrine levels.

*, $P<0.01$ as compared with control rats

	Control rats (n = 7)	Stressed rats (n = 7)
Plasma levels (nM)		
Epinephrine	43.6 ± 3.2	62.8 ± 2.3*
Norepinephrine	364.4 ± 12.5	495.2 ± 15.8*
Adrenal levels (nmole/mg protein)		
Epinephrine	27.8 ± 1.0	20.5 ± 1.1*
Norepinephrine	4.8 ± 0.2	2.9 ± 0.2*

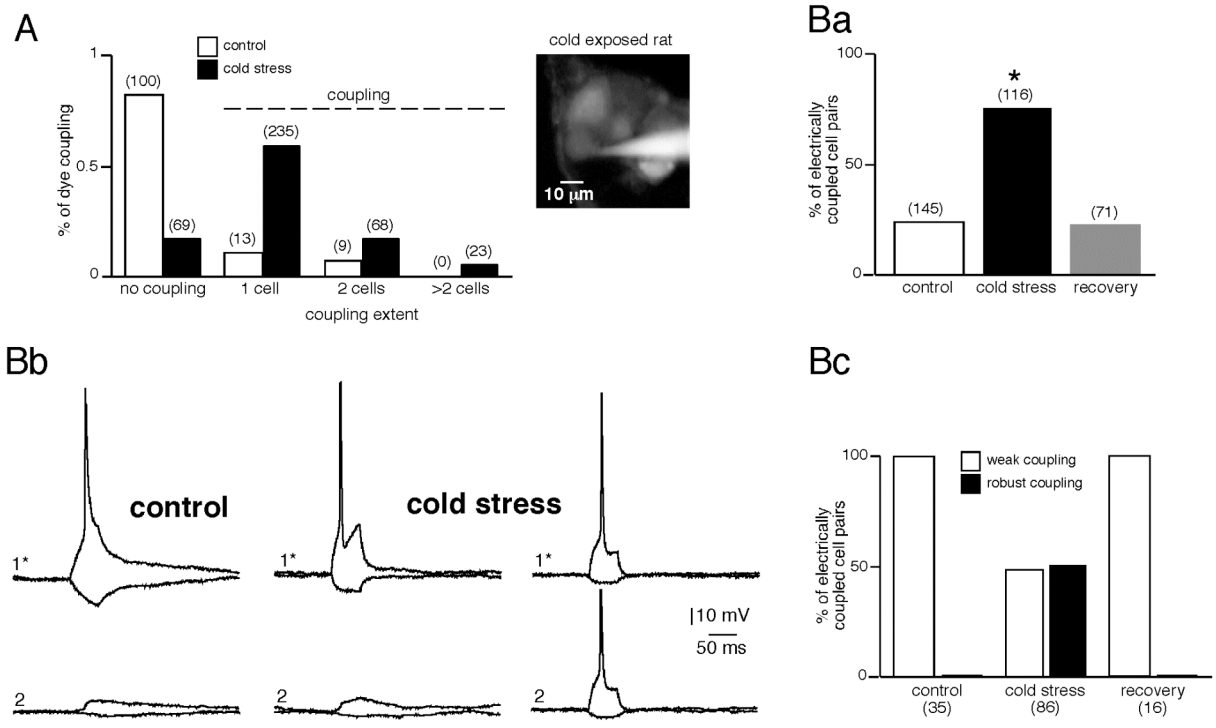
A
control
cold stress
% of dye coupling
1
0.5
0
(100)
(69)
(13)
(235)
(9)
(68)
(0)
(23)
coupling
no coupling
1 cell
2 cells
>2 cells
coupling extent
cold exposed rat
10 µm
Ba
% of electrically coupled cell pairs
100
50
0
(145)
*
(116)
(71)
control
cold stress
recovery
Bb
control
cold stress
1*
2
10 mV
50 ms
Bc
% of electrically coupled cell pairs
100
50
0
weak coupling
robust coupling
control (35)
cold stress (86)
recovery (16)

FIGURE 1

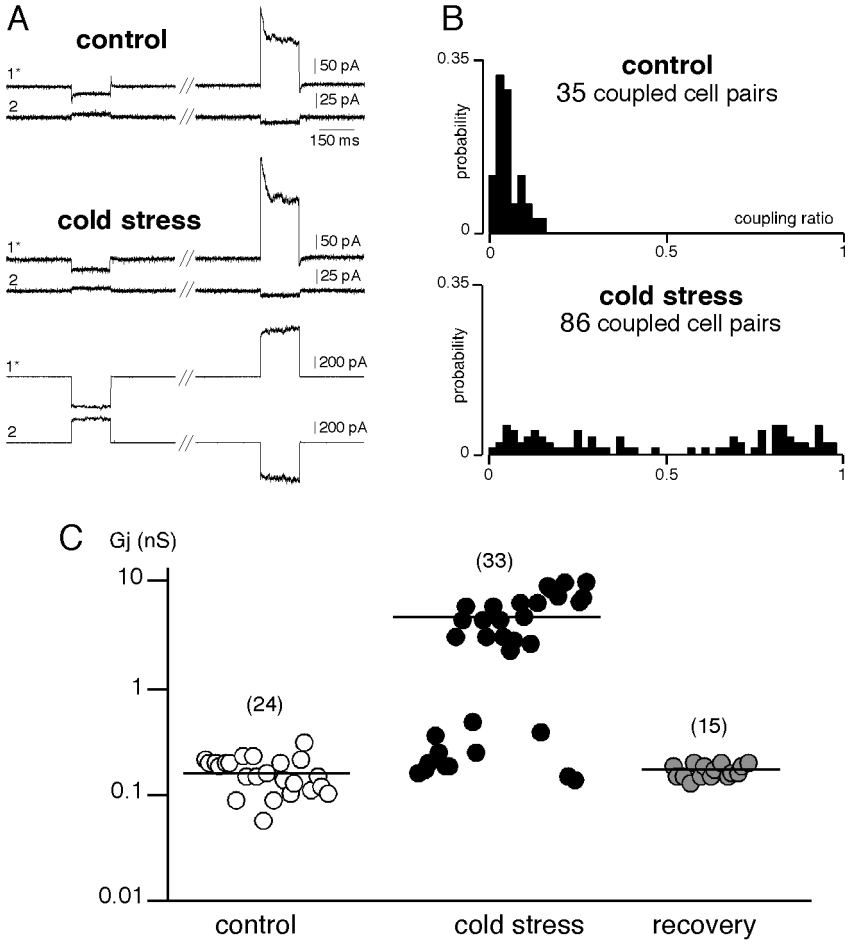
A
control
1*
2
50 pA
25 pA
150 ms
cold stress
1*
2
50 pA
25 pA
1*
2
200 pA
200 pA
B
control
35 coupled cell pairs
probability
0.35
0
0
0.5
1
coupling ratio
cold stress
86 coupled cell pairs
probability
0.35
0
0
0.5
1
C
Gj (nS)
10
1
0.1
0.01
(24)
(33)
(15)
control
cold stress
recovery

FIGURE 2

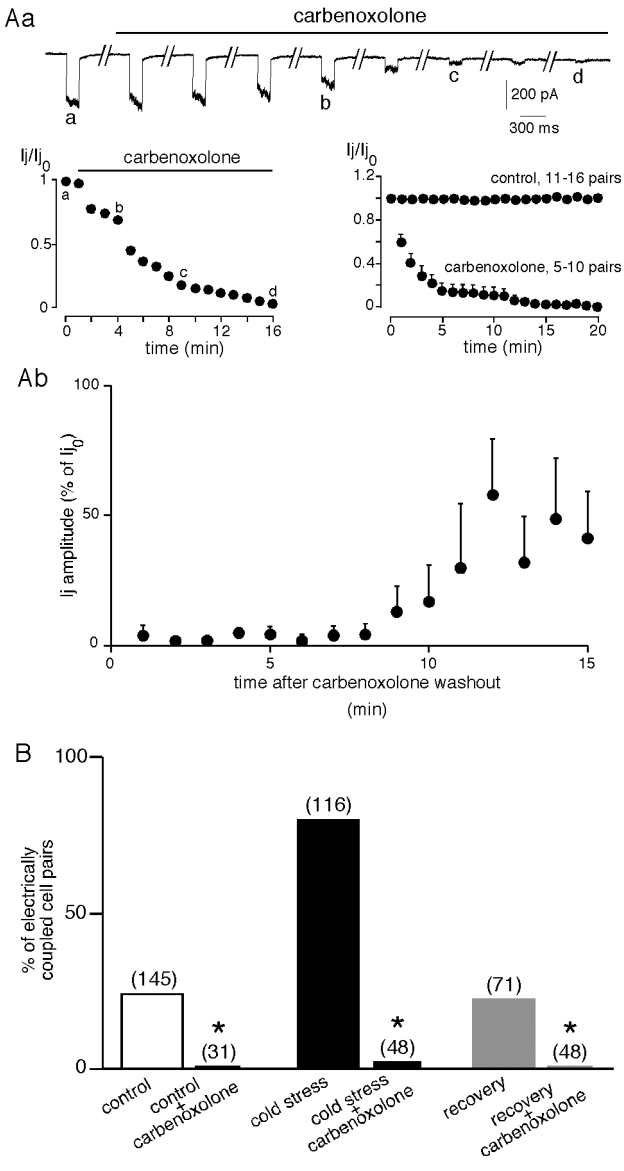
Aa
carbenoxolone
200 pA
300 ms
a
b
c
d
Ij/Ij0
carbenoxolone
time (min)
control, 11-16 pairs
carbenoxolone, 5-10 pairs
Ab
Ij amplitude (% of Ij0)
time after carbenoxolone washout
(min)
B
% of electrically coupled cell pairs
(145)
(31)
(116)
(48)
(71)
(48)
control
control + carbenoxolone
cold stress
cold stress + carbenoxolone
recovery
recovery + carbenoxolone

FIGURE 3

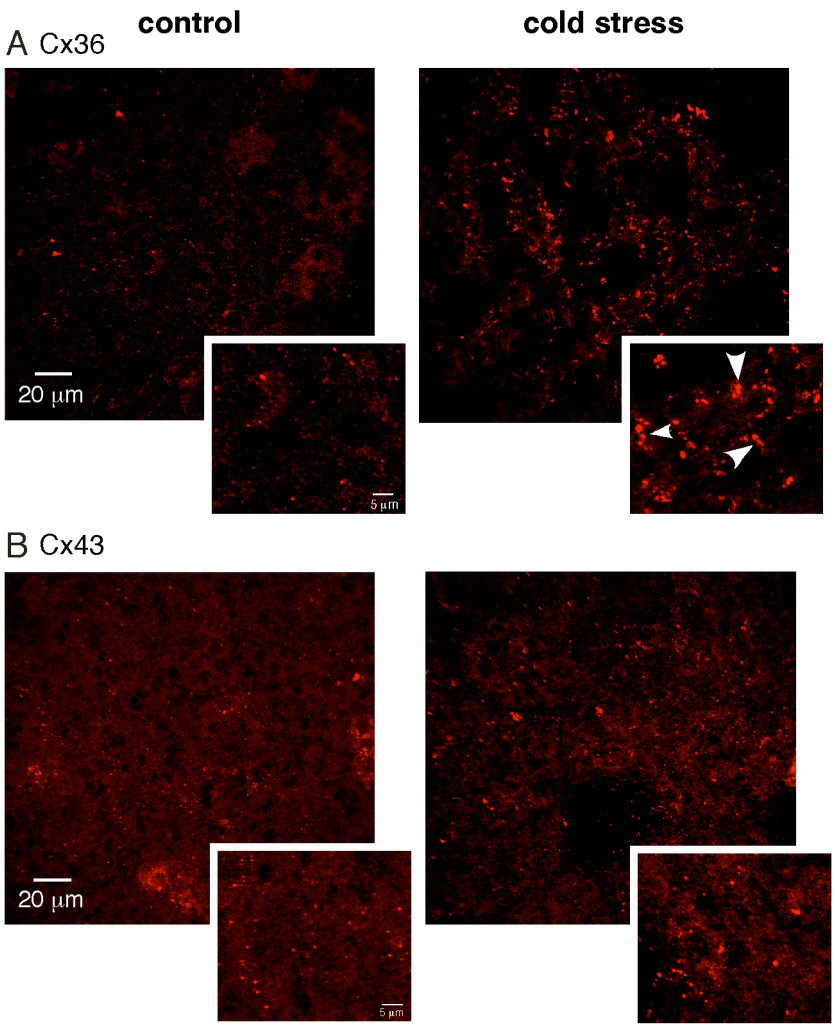

FIGURE 4

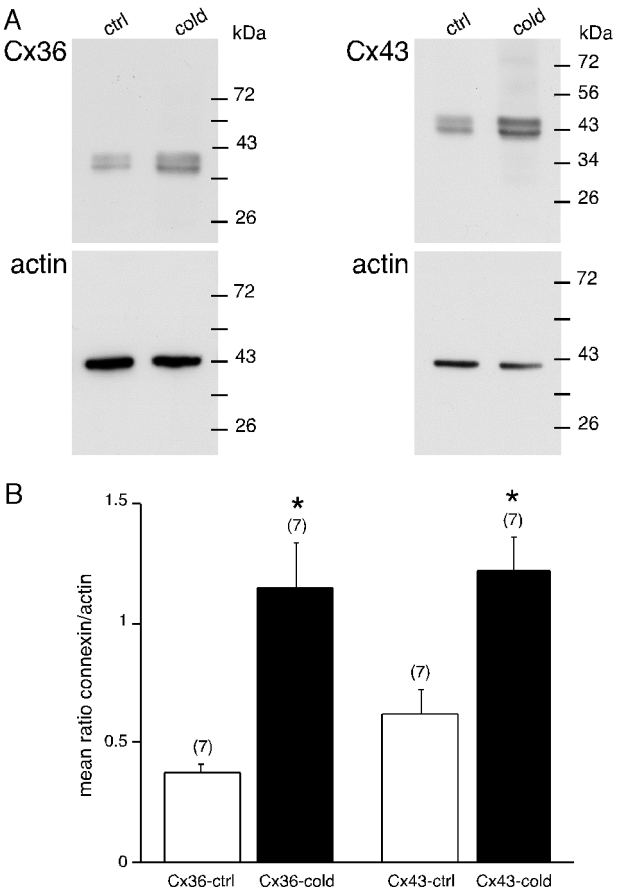
A
Cx36
ctrl
cold
kDa
72
43
26
actin
72
43
26
Cx43
ctrl
cold
kDa
72
56
43
34
26
actin
72
43
26
B
mean ratio connexin/actin
1.5
1
0.5
0
*
(7)
(7)
*
(7)
(7)
Cx36-ctrl
Cx36-cold
Cx43-ctrl
Cx43-cold

FIGURE 5

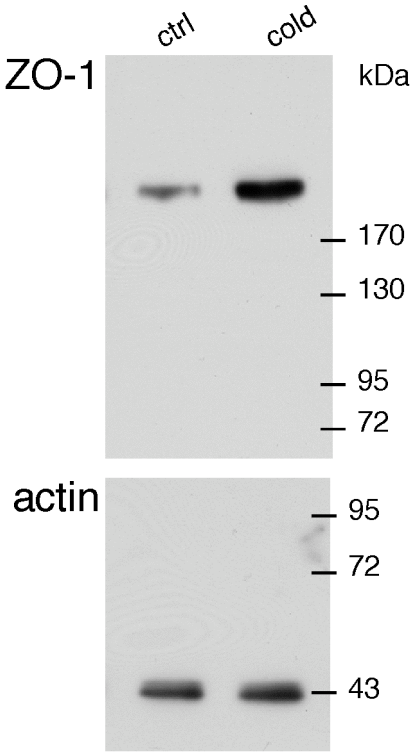

FIGURE 6

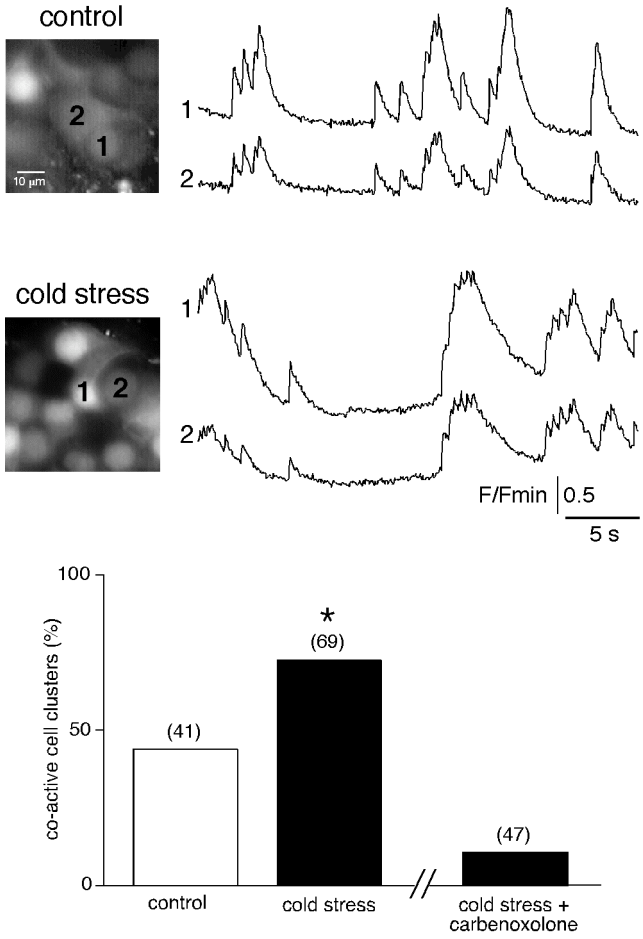
control
2
1
10 µm
1
2
cold stress
1
2
1
2
F/Fmin
0.5
5 s
100
50
0
co-active cell clusters (%)
(41)
*
(69)
(47)
control
cold stress
cold stress +
carbenoxolone

FIGURE 7

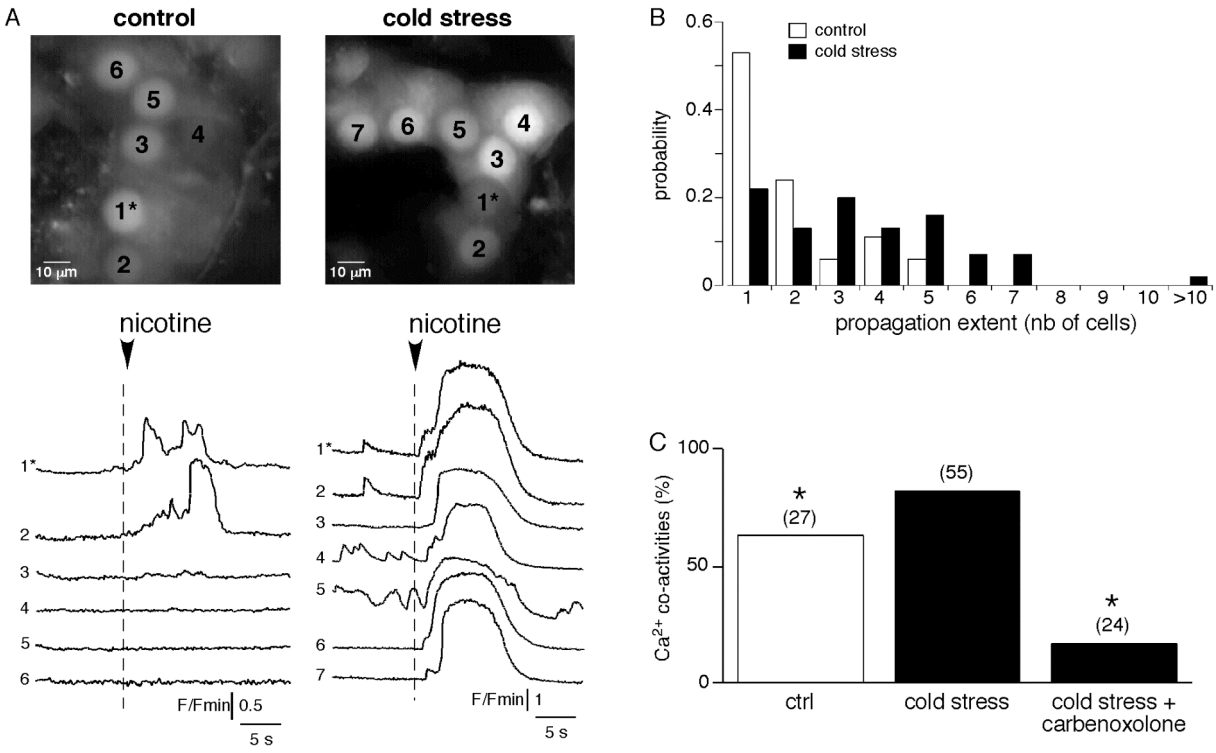
A
control
cold stress
6
5
4
3
1*
2
10 µm
7
6
5
4
3
1*
2
10 µm
nicotine
nicotine
1*
2
3
4
5
6
F/Fmin 0.5
5 s
1*
2
3
4
5
6
7
F/Fmin 1
5 s
B
control
cold stress
probability
0.6
0.4
0.2
0
1
2
3
4
5
6
7
8
9
10
>10
propagation extent (nb of cells)
C
Ca2+ co-activities (%)
100
50
0
*
(27)
(55)
*
(24)
ctrl
cold stress
cold stress +
carbenoxolone

FIGURE 8